PLOS Biology

SHORT REPORTS

SGO2 does not play an essential role in separase inhibition during meiosis I in mouse oocytes

Benjamin Wetherall[1], **David Bulmer**[2], **Alexandra Sarginson**[1], **Christopher Thomas**[3*], **Suzanne Madgwick**[1*]

1 Faculty of Medical Sciences, Biosciences Institute, Newcastle University, Newcastle, United Kingdom, **2** Bioimaging Unit, Faculty of Medical Sciences, Newcastle University, Newcastle, United Kingdom, **3** IBDM—Institut de Biologie du Développement de Marseille, CNRS—UMR 7288, Aix-Marseille Université, Marseille, France

* christopher.thomas@univ-amu.fr (CT); suzanne.madgwick@newcastle.ac.uk (SM)

Citation: Wetherall B, Bulmer D, Sarginson A, Thomas C, Madgwick S (2025) SGO2 does not play an essential role in separase inhibition during meiosis I in mouse oocytes. PLoS Biol 23(4): e3003131. https://doi.org/10.1371/journal.pbio.3003131

Academic Editor: Jonathon Pines, The Institute of Cancer Research, UNITED KINGDOM OF GREAT BRITAIN AND NORTHERN IRELAND

Received: February 3, 2025

Accepted: March 25, 2025

Published: April 23, 2025

Data availability statement: All relevant data are within the paper and its Supporting information files.

Funding: This work was supported by an MRC (UKRI | Medical Research Council) Career Development Award to S.M. [MR/T010789/1].

Abstract

During meiosis I in oocytes, anaphase is triggered by deactivation of cyclin B1-CDK1 and activation of separase. Active separase plays an essential role in cleaving cohesin rings that hold homologous chromosomes together. Critically, separase must be inhibited until all chromosomes are aligned and the cell is prepared for anaphase I. Inhibition can be mediated through the binding of separase to either securin or cyclin B1-CDK1. The relative contribution of each inhibitory pathway varies depending on cell type. Recently, shugoshin-2 (SGO2) has also been shown to inhibit separase in mitotic cells. Here, we used a separase biosensor and perturbed the three inhibitory pathways during meiosis I in mouse oocytes. We show that inhibition mediated by either securin or cyclin B1-CDK1, but not SGO2, is independently sufficient to suppress separase activity. However, when both the securin and cyclin B1-CDK1 inhibitory pathways are perturbed together, separase activity begins prematurely, resulting in gross segregation defects. Furthermore, we characterized SGO2 destruction dynamics and concluded that it is not an essential separase inhibitor in mouse oocytes. The existence of multiple separase inhibitory pathways highlights the critical importance of tightly regulated separase activity during this unique and challenging cell division.

Introduction

Meiosis is the specialized cell division that generates female and male gametes, the egg and sperm. In meiosis I, chromosomes are organized in a structure known as a bivalent. The bivalent is composed of two homologous chromosomes of different parental origin [1]. Both homologous chromosomes within the bivalent, as well as the sister chromatids within each homolog, are held together by a ring-like protein complex known as cohesin [2].

https://www.ukri.org/councils/mrc/ The funder played no role in the study design, data collection and analysis, decision to publish, or preparation of the manuscript.

Competing interests: The authors have declared that no competing interests exist.

Abbreviations: BSA, Bovine Serum Albumin; MO, morpholino oligo; NEBD, post-nuclear envelope breakdown; PBS, phosphate-buffered saline; SAC, spindle assembly checkpoint; SGO2, shugoshin-2.

For correct progression through the meiotic divisions, cohesin must be removed in distinct steps. In meiosis I, cohesin is cleaved from chromosome arms—allowing the homologous chromosomes within each bivalent to segregate. In meiosis II, cohesin still present at the pericentromeric regions of chromosomes is cleaved—allowing sister chromatids to separate [3]. In both divisions, the protease separase plays an essential role, by cleaving the meiosis-specific kleisin subunit of cohesin—REC8 [4–6]. It is therefore critical that separase is carefully regulated through both divisions and only becomes active once chromosomes are aligned and prepared to divide.

In mouse oocytes, two inhibitory pathways have been implicated in separase inhibition. In the first pathway, separase directly interacts with securin, which acts as a pseudosubstrate inhibitor of separase [7–13]. Additionally, upon phosphorylation by CDK1, separase is inhibited by binding CDK1's activating partner cyclin B1 [14–17]. The binding of separase with either securin or cyclin B1 is mutually exclusive, and the relative contribution of each pathway varies depending on cell type and developmental state [15,17]. For example, in female mouse meiosis II and eukaryotic mitosis, securin is largely responsible for separase inhibition, while primordial germ cells and early-stage embryos rely primarily on cyclin B1-CDK1-mediated separase inhibition [18–20]. Interestingly however, while securin binding to separase is the primary inhibitory mechanism in mitotic cells, it is also dispensable, demonstrating the compensatory nature of these two pathways [21–23]. Similarly, in meiosis I mouse oocytes, Chiang and colleagues only observed chromosome segregation errors when both securin- and cyclin B1-CDK1-mediated separase inhibition were perturbed together [24]. However, in this study, separase activity was not measured directly, and it remains unclear when and how these segregation defects arise.

Shugoshin-2 (SGO2) has also recently been shown to have the capacity to inhibit separase in mitotic cells [25]. This work demonstrates that on association with spindle assembly checkpoint (SAC)-activated MAD2, SGO2 can sequester the majority of free separase in securin knock-out cells. Like securin, through a pseudosubstrate sequence within its N-terminus, SGO2 can bind directly to the active site of separase, blocking its protease activity. It is currently unknown whether SGO2-MAD2 contributes to separase inhibition during oocyte meiosis. When we consider that securin and cyclin B1-CDK1 are regulated differently in oocytes compared to mitosis [26,27], it is important to investigate whether SGO2 might contribute to separase inhibition during this specialized division.

Therefore, while we have some understanding of the pathways regulating separase in mouse oocytes, exactly how these proteins work together to keep separase activity at bay through the extended duration of meiosis I remains unclear.

In this study, we set out to address the question of separase regulation in mouse oocytes using a live-cell imaging approach. We utilized a fluorescent biosensor to visualize separase activity, in combination with strategies to perturb key cell cycle proteins of interest. We add dynamic understanding to previous findings that either securin- or cyclin B1-CDK1-mediated inhibition is independently sufficient to suppress separase activity in oocyte meiosis I. When both compensatory pathways

are disrupted in tandem, separase activity initiates up to 1 h ahead of anaphase I and is accompanied by gross segregation defects. We additionally investigated the destruction dynamics of SGO2 in mouse oocytes and determined that it is unlikely to function as a separase inhibitor in unperturbed oocytes. The existence of multiple layers of redundancy and crosstalk between separase inhibitory pathways emphasizes the crucial role of precisely regulated separase activity in coordinating oocyte meiosis successfully.

Results

Both securin- and cyclin B1-CDK1-mediated inhibition are independently sufficient to suppress separase activity in meiosis I

We set out to investigate the pathways regulating separase activity in mouse oocytes. To do this, we used strategies to inhibit the known meiotic separase inhibitors securin and cyclin B1-CDK1 to assess their contributions. Chiang and colleagues previously showed that segregation errors in fixed meiosis II oocytes were only observed when both securin- and cyclin B1-CDK1-mediated separase inhibition were removed [24]. However, when these errors arise and how separase is regulated through time remain unclear. To investigate this, we used a live separase activity biosensor generated by Nam and colleagues which has been validated in HeLa cells, U2OS cells, mouse embryonic fibroblasts, and mouse oocytes [28–31]. The sensor is composed of a nucleosome-targeted H2B protein that is fused to eGFP and mCherry fluorophores. Active separase cleaves an Scc1 peptide sequence located between the two fluorophores (Fig 1a). This cleavage leads to a shift in fluorescence from yellow to red, as the eGFP signal dissociates into the cytoplasm while mCherry remains attached to histones linked to chromosomal DNA (Fig 1b). We chose to use the Scc1 separase biosensor due to the pronounced fluorescence change, making quantification of cleavage timings most reliable. However, we first confirmed that the Scc1 sensor cleavage takes place with the same timing as the Rec8 sensor in mouse oocytes (Fig 1b).

We first used the Scc1 separase sensor in combination with knockdown of securin by morpholino oligo (MO) such that in prometaphase I, MO oocytes contained ~13% of the protein level relative to non-treated control oocytes (as previously quantified by western blot [26]). Despite severe depletion of securin, the cleavage activity of separase was still restricted to the final 30 min before polar body extrusion (Fig 1ci). This result agrees with observations made in fixed oocytes, suggesting that cyclin B1-CDK1 is sufficient to compensate for the loss of securin [24]. To test whether the reverse is also true, we injected oocytes with a previously published separase AA mutant [24]. This construct is fully active but lacks CDK1 phosphorylation sites (S1121A and T1342A) that prevent its inhibition by cyclin B1-CDK1. By this strategy, cyclin B1-CDK1-mediated separase inhibition is perturbed without affecting other crucial functions of cyclin B1-CDK1 in meiosis. Importantly, oocytes expressing separase AA produce separase activity profiles identical to control oocytes, suggesting that securin was similarly sufficient to compensate for a loss of cyclin B1-CDK1-mediated inhibition (Fig 1cii). In contrast, where securin protein levels are restricted in separase AA-expressing oocytes (securin MO + separase AA), cleavage activity is detected up to 1 h ahead of control oocytes (Fig 1ciii). Furthermore, securin MO + separase AA oocytes have a significantly greater total cleavage compared to control oocytes (Fig 1d). The difference in cleavage timing is also apparent in the confocal microscopy images, where the eGFP signal remains high on chromosomes in control oocytes until just prior to chromosome segregation. In contrast, in securin MO + separase AA oocytes, the eGFP signal begins to visibly decrease approximately 30 min earlier (S1b Fig). Importantly, this premature separase activity was specific to the loss of both securin- and cyclin B1-CDK1-mediated inhibition, and not due to separase overexpression in the absence of securin. Oocytes treated with securin MO + an excess of wild-type separase have cleavage timings identical to control oocytes (Fig 1civ), suggesting that cyclin B1-CDK1 alone has the capacity to inhibit an abundance of separase. Despite the premature separase activity in securin MO + separase AA oocytes, we observed no change in the timing of polar body extrusion (Fig 1e), likely due to the inefficient nature of the SAC in oocytes [32].

To monitor the impact of premature separase activity in securin MO + separase AA oocytes, we used confocal microscopy to image live oocytes stained with SiR-DNA to track individual chromosome movements. This analysis revealed

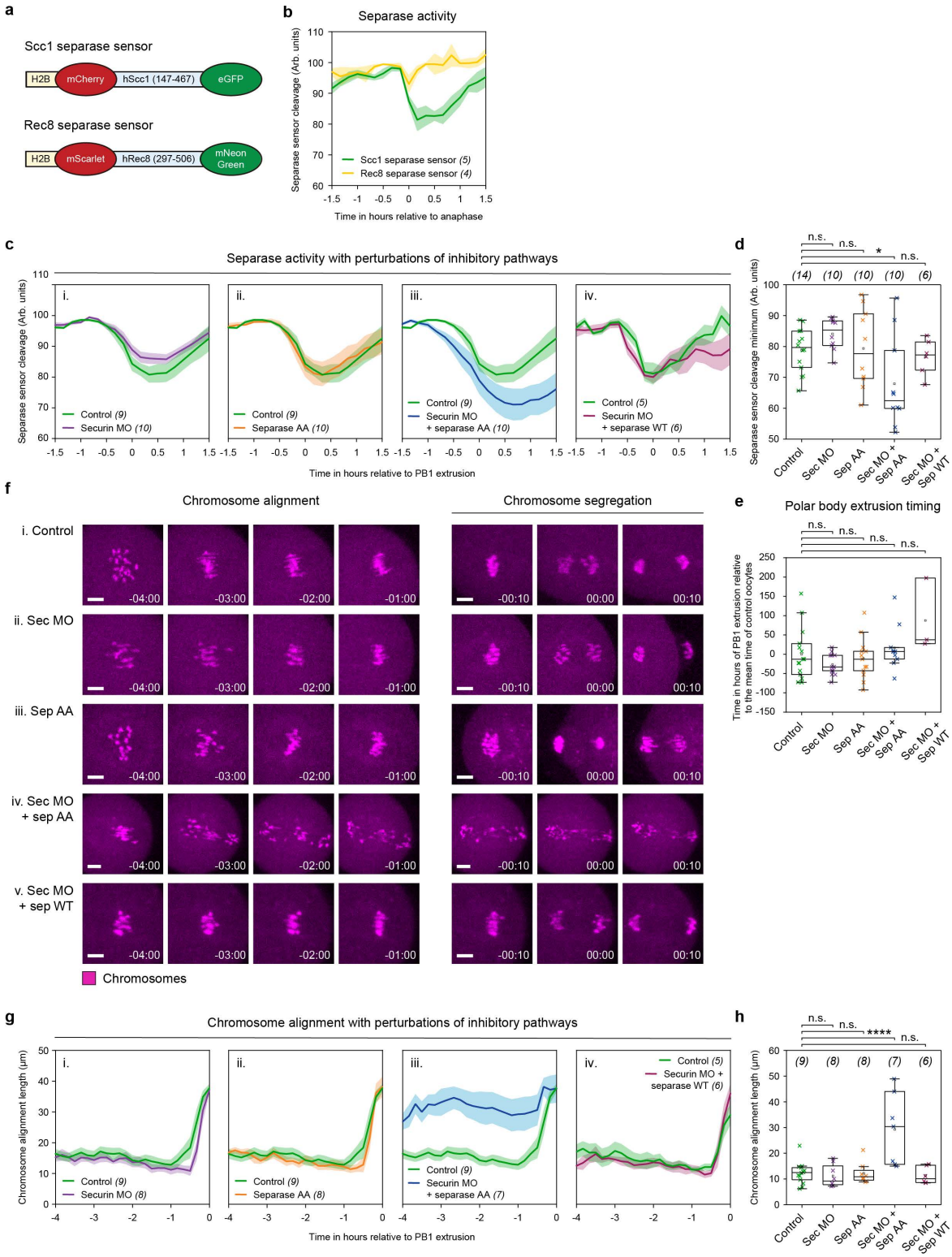

Fig 1. Both securin- and cyclin B1-CDK1-mediated inhibition are independently sufficient to suppress separase activity in meiosis I. **(a)** Schematic diagrams of H2B-mCherry-hScc1-eGFP and H2B-mScarlet-hRec8-mNeonGreen separase activity biosensors. **(b)** Graph comparing Scc1 (green trace, *n* = 5) and Rec8 (yellow trace, *n* = 4) separase sensor detection in oocytes aligned at PB1 extrusion. **(c)** Graphs showing mean

MI separase activity profiles as determined by the Scc1 separase sensor (eGFP/mCherry ratio) for control oocytes (green trace, *n* = 9) compared to **(i)** securin MO oocytes (purple trace, *n* = 10), **(ii)** separase AA oocytes (orange trace, *n* = 10), and **(iii)** securin MO + separase AA oocytes (blue trace, *n* = 10). To control for overexpression of separase in (iii), **(iv)** directly compares securin MO + separase WT oocytes (burgundy trace, *n* = 6) with control oocytes (green trace, *n* = 5). **(d)** Quantification of separase sensor cleavage minimum in control (green crosses, *n* = 14), securin MO (purple crosses, *n* = 10), separase AA (orange crosses, *n* = 10), securin MO + separase AA (blue crosses, *n* = 10), and securin MO + separase WT (burgundy crosses, *n* = 6) oocytes. Crosses represent individual oocytes. **(e)** Quantification of polar body extrusion timings in oocyte treatment groups as per part (c, d). Timings are presented relative to the mean polar body extrusion time (0) in control oocytes. **(f)** Representative images showing chromosome alignment and segregation in **(i)** control, **(ii)** securin MO, **(iii)** separase AA, **(iv)** securin MO + separase AA, and **(v)** securin MO + separase WT oocytes. Time relative to PB1 extrusion. Chromosomes were visualized by incubating oocytes with SiR-DNA (magenta). Scale bar = 10 μm. **(g)** Graphs showing the maximum distance between chromosomes, measured axial to the spindle per 10-minute time points over 4 h prior to PB1 extrusion. Comparing control oocytes (green traces, *n* = 9) with **(i)** securin MO (purple trace, *n* = 8), **(ii)** separase AA (orange trace, *n* = 8), **(iii)** securin MO + separase AA (blue trace, *n* = 7), and **(iv)** securin MO + separase WT (burgundy trace, *n* = 6) oocytes. **(h)** Quantification of chromosome alignment length in individual oocytes 1 h before PB1 extrusion in treatment groups as in panel (g). Crosses represent individual oocyte measurements. In panels: (b), (c), and (g): thick lines show the mean data, lighter shadows show the SEM. In panels (d), (e), and (h): ****$P < 0.0001$, ***$P < 0.001$, **$P < 0.01$, *$P < 0.1$, n.s. = non-significant, two-sided unpaired *t* test; box = 25%–75%, whiskers = 0%–100%, center = median, center box = mean. All source data can be found in the S1 Data spreadsheet.

https://doi.org/10.1371/journal.pbio.3003131.g001

severe defects in chromosome alignment and segregation in securin MO + separase AA oocytes (Fig 1fiv). Additionally, quantification of the maximum distance between chromosomes in each 10-min time interval prior to polar body extrusion showed significantly more disorganized metaphase plates during meiosis I chromosome alignment in securin MO + separase AA oocytes (Fig 1g). Notably, this analysis also revealed that 1 h prior to PB1 extrusion, even before detectable cleavage of the sensor begins, the average length of the chromosome plate in securin MO + separase AA oocytes was significantly longer (29.2 ± 5.3 μm; Fig 1h) than in control oocytes (12.3 ± 1.1 μm; Fig 1h). In contrast, securin MO (11.2 ± 1.5 μm; Fig 1h), separase AA (12.2 ± 1.5 μm; Fig 1h), and securin MO + separase WT (11.4 ± 1.4 μm; Fig 1h) oocytes were the same as controls.

These data further demonstrate that either inhibitory pathway, securin or cyclin B1-CDK1, is sufficient to prevent premature separase activity in mouse oocyte meiosis I. When both pathways are perturbed in the same oocyte, the timings of anaphase I onset and separase release become uncoupled, resulting in severe defects in chromosome alignment and segregation.

Shugoshin-2 is targeted for degradation by the APC/C in anaphase I

While the defects observed in securin MO + separase AA oocytes were severe, we found it curious that even when both inhibitory pathways were perturbed, detectable cleavage of the sensor was only observed in the final 1.5 h before polar body extrusion (Fig 1ciii). We therefore wanted to investigate whether another inhibitory mechanism may be functioning in these oocytes. Specifically, SGO2, recently shown to be capable of separase inhibition in human mitotic cells when securin was knocked-out [25].

SGO2 contains a conserved pseudosubstrate sequence within its N-terminus (Fig 2a) that can directly bind the active site of separase, blocking its protease activity [25]. We hypothesized that SGO2 may be contributing to separase inhibition in securin MO + separase AA oocytes, and the release of separase activity around 1.5 h ahead of polar body extrusion in these oocytes (Fig 1ciii) may reflect a time when the inhibitory capacity of SGO2 is lost. We further hypothesized that this loss may be due to SGO2 being targeted for proteasomal degradation by the APC/C, like securin, cyclin B1, and indeed its homolog SGO1 [33–35]. To support this hypothesis, when we compared multiple sequence alignments of SGO2, we identified several conserved APC/C destruction motifs [36] (Fig 2a). Specifically, the N-terminus of SGO2 contains a previously undescribed KEN box [37], TEK box [38], and D-box [39] just upstream of the separase pseudosubstrate motif identified by Hellmuth and colleagues [25]. To further investigate whether SGO2 is targeted for destruction during meiosis I, we measured SGO2 protein levels in oocytes using a live fluorescent SGO2 reporter. We observed that the SGO2 reporter was rapidly degraded late in meiosis I, only 30 min ahead of PB1 extrusion and over an hour later than both securin and cyclin B1 destruction is initiated (Fig 2b). We then confirmed that the timing of SGO2 degradation is unchanged between

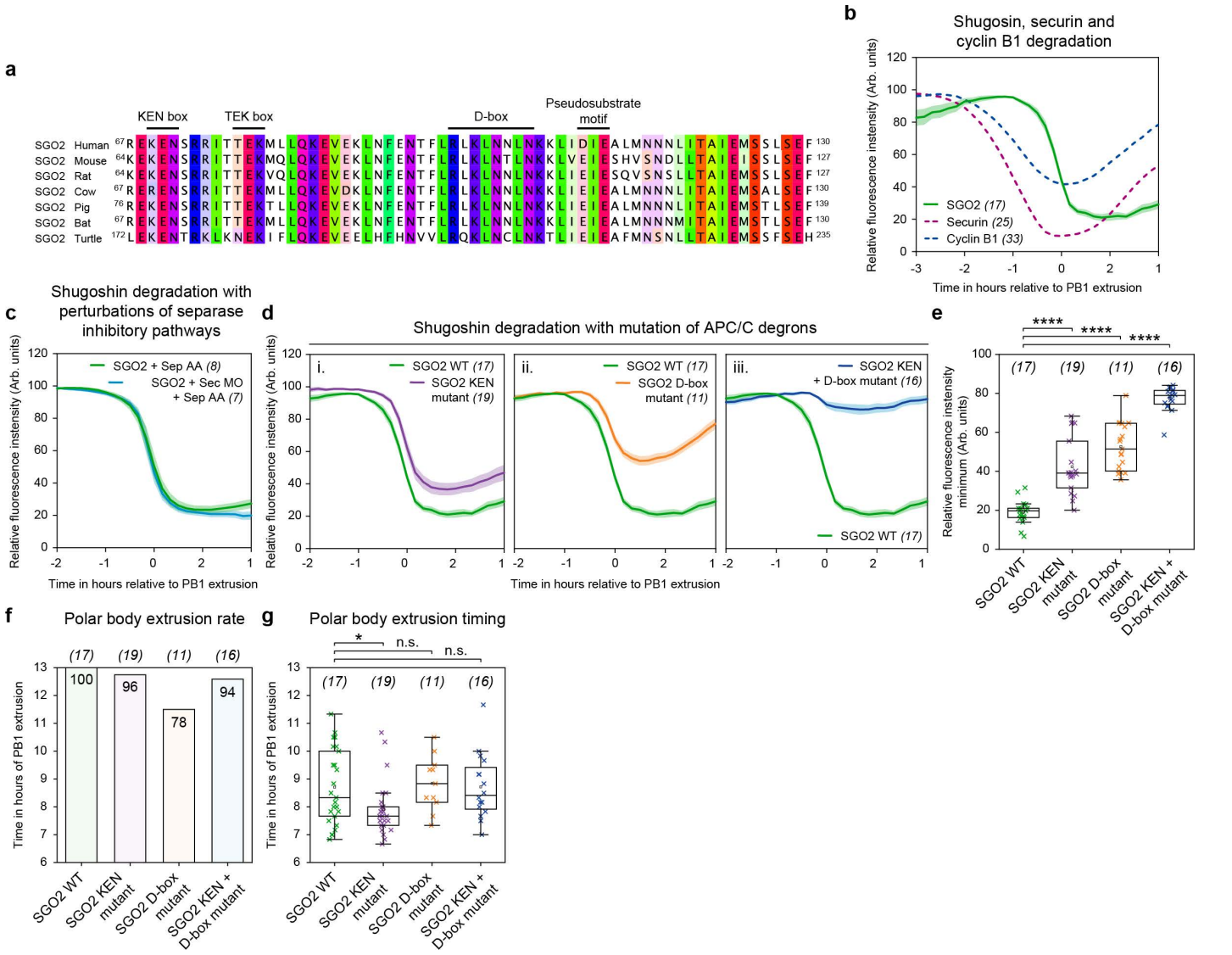

Fig 2. Shugoshin-2 (SGO2) is targeted for degradation by the APC/C in anaphase I. (a) Multiple sequence alignment of the N-terminal segments in SGO2 orthologs containing the KEN box, TEK box, D-box, and separase pseudosubstrate motif. **(b)** Mean SGO2 (green trace, *n* = 17), securin (burgundy dashed trace, *n* = 25), and cyclin B1 (blue dashed trace, *n* = 33) destruction profiles relative to PB1 extrusion. **(c)** Mean SGO2 destruction traces comparing oocytes with separase AA expression (green trace, *n* = 8) and securin MO + separase AA expression (blue trace *n* = 7). **(d)** SGO WT destruction traces relative to PB1 extrusion (green trace, *n* = 17) compared to **(i)** SGO2 KEN mutant (purple trace *n* = 19), **(ii)** SGO2 D-box mutant (orange trace, *n* = 11), and **(iii)** SGO2 KEN + D-box mutant (blue trace, *n* = 16). **(e)** Quantification of relative degradation by fluorescence intensity minimum for groups in panel (d). Crosses represent individual oocyte measurements. Plots **(f)** and **(g)** display polar body extrusion rates and polar body extrusion timings respectively for groups in panels (d) and (e). In panels (b), (c), and (d): thick lines show the mean data, lighter shadows show the SEM. In panels (e) and (g): ****$P < 0.0001$, ***$P < 0.001$, **$P < 0.01$, *$P < 0.1$, n.s. = non-significant, two-sided unpaired *t* test; box = 25%–75%, whiskers = 0%–100%, center = median, center box = mean. All source data can be found in the S1 Data spreadsheet.

https://doi.org/10.1371/journal.pbio.3003131.g002

control and securin MO + separase AA oocytes (Fig 2c). This late destruction suggests that SGO2 is not mediating separase inhibition in securin MO + separase AA oocytes, as SGO2 is still present at high levels for over an hour after the point of premature separase activation (Fig 1ciii) [25].

Interestingly, when we mutated the KEN box and D-box, which had an additive effect in stabilizing SGO2 during anaphase I (Fig 2d and 2e), this had no impact on the polar body extrusion rate or timing (Fig 2f and 2g). This suggests

that unlike in securin and cyclin B1 [40], KEN/D-box mutants of SGO2 are unable to block anaphase onset and polar body extrusion through persistent separase inhibition in mouse oocytes. However, due to the close vicinity of the KEN box and D-box to the separase-interacting pseudosubstrate motif in SGO2 (Fig 2a), we cannot discount that these mutants fail to block progression into meiosis II due to an impaired capacity to interact with separase. Furthermore, in mitotic cells, release of separase from SGO2-mediated inhibition occurs in an APC/C-independent manner [25]. We therefore looked for an additional approach to assess the impact of SGO2 on separase inhibition in oocytes.

Shugoshin-2 is not essential for separase inhibition in meiosis I

Using a MO, we knocked down SGO2 such that 3 h after post-nuclear envelope breakdown (NEBD), MO oocytes contained <15% of the protein level of non-treated control oocytes (as quantified by immunofluorescence; S2a and S2b Fig). Even with this depletion of SGO2 protein, like in control oocytes, the cleavage activity of separase remained restricted to the final 30 min preceding PB1 extrusion (Fig 3ai). We additionally injected oocytes with SGO2 MO + securin MO (Fig 3aii) and SGO2 MO + separase AA (Fig 3aiii). In both of these double perturbations, the cleavage timing was consistent with that observed in control oocytes. Together, these data provide important evidence that in unperturbed mouse oocytes, SGO2 does not play an essential role in the inhibition of separase during meiosis I.

We next wanted to revisit the idea that in securin MO + separase AA oocytes, SGO2 may be able to compensate for the loss of securin- and cyclin B1-CDK1-mediated separase inhibition prior to becoming active in the final 1.5 h before PB1 extrusion. To address this, we knocked down both SGO2 and securin protein levels in separase AA-expressing oocytes (SGO2 MO + securin MO + separase AA). In these oocytes, the loss of SGO2 had no further impact on the timing of cleavage activity, which still initiates up to 1.5 h ahead of PB1 extrusion, like that of securin MO + separase AA oocytes (Fig 3aiv). However, there was a marked change in the extent to which the sensor was cleaved in SGO2 MO + securin MO + separase AA oocytes, now significantly reduced (Fig 3b), and accompanied by a delay in PB1 extrusion (Fig 3c).

To monitor the impact of premature separase activity in SGO2 MO + securin MO + separase AA oocytes, we imaged live oocytes stained with SiR-DNA to track individual chromosome movements. This analysis revealed errors in chromosome alignment and segregation (Fig 3dv) comparable to securin MO + separase AA oocytes (Fig 1fi). In addition, in SGO2 MO + securin MO + separase AA oocytes, the length of the chromosome plate 1 h prior to PB1 extrusion (30.6 ± 5.6 μm) was double that in control oocytes (14.7 ±1 μm; Fig 3e and 3f) and almost identical to that of securin MO + separase AA oocytes (Fig 1h).

In conclusion, these findings, along with the destruction timings shown in Fig 2, provide compelling evidence that SGO2 does not play an essential role in separase inhibition during meiosis I in mouse oocytes.

Discussion

Accurate progression through meiosis in oocytes requires the timely removal of key cell cycle proteins. From prometaphase I, the removal of cyclin B1 and securin are synchronous, ensuring that CDK1 activity loss is coupled to separase release. Importantly, while the two events are connected, loss of CDK1 activity initiates ahead of separase activation by approximately 30 min [27]. This ordering ensures that separase is not released until the cell has committed to anaphase. Aberrant separase release ahead of this time point could have severe consequences. Indeed, in securin MO + separase AA oocytes, separase activity initiates at the same time as the loss in CDK1 activity in unperturbed oocytes, resulting in significant segregation defects [27].

While cyclin B1-CDK1 drives many diverse processes as a master cell cycle regulator in mitosis and meiosis [41,42], securin has been shown to primarily function as a separase inhibitor [43]. Both must be depleted to release separase activity during exit from meiosis I [24,40]. Importantly; however, cyclin B1 and securin are only partially degraded, and some CDK1 activity remains during meiosis I exit in mouse oocytes [26,27]. This situation is intrinsic to the production of a haploid MII oocyte. Complete cyclin B1-CDK1 activity loss would drive the oocyte into S-phase [44], while complete loss

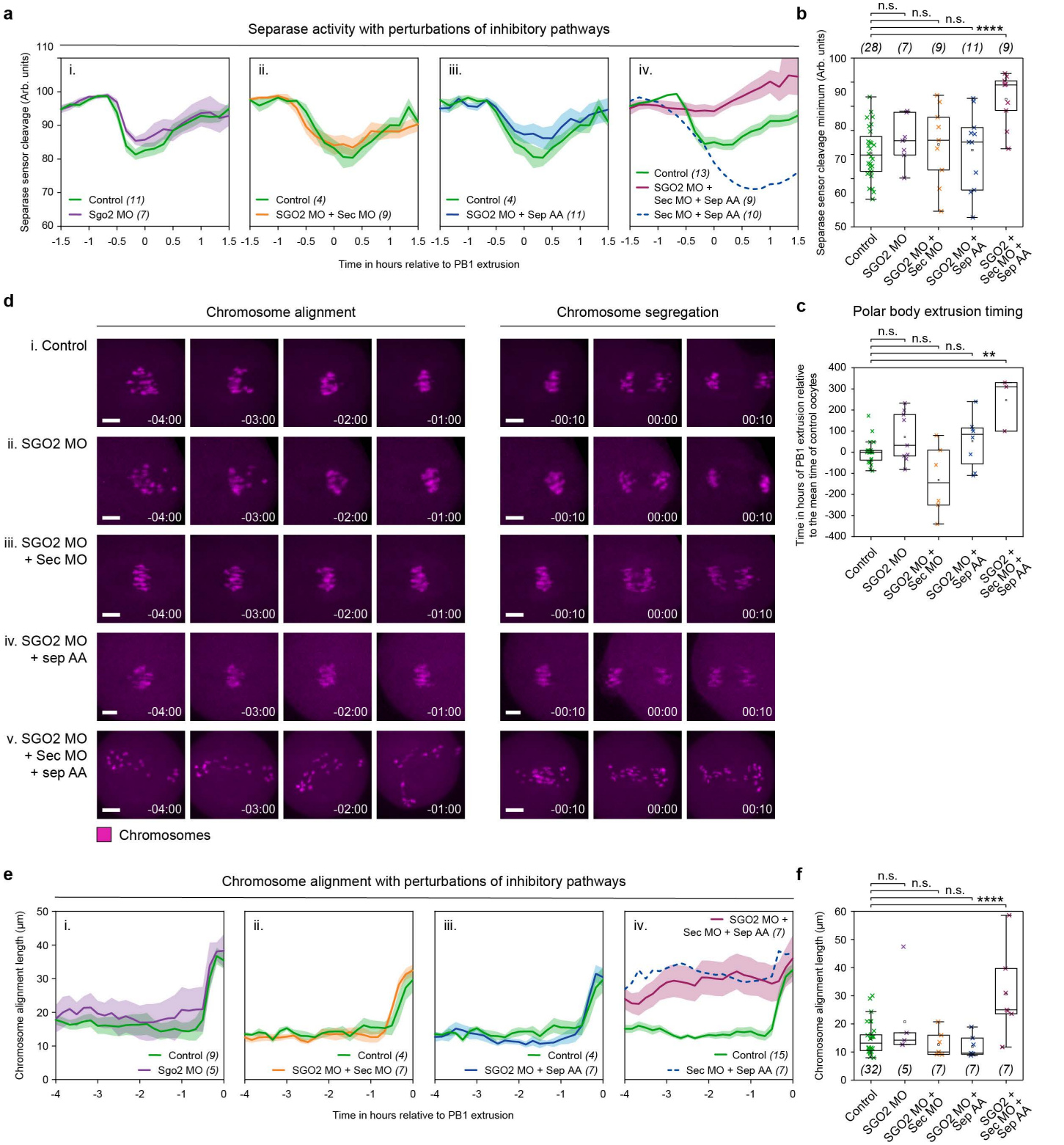

Fig 3. Shugoshin-2 (SGO2) is not essential for separase inhibition in meiosis I. (a) Graphs showing mean MI separase activity profiles as determined by the Scc1 separase sensor (eGFP/mCherry ratio) for control oocytes (green trace, *n* = 11) compared to **(i)** SGO2 MO (purple trace, *n* = 7), **(ii)** SGO2 MO + securin MO (orange trace, *n* = 9), **(iii)** SGO2 MO + separase AA (blue trace, *n* = 11), and **(iv)** SGO2 MO + securin MO + separase AA

oocytes (burgundy trace, *n* = 9). In part (iv) a dashed dark blue line is included for comparison, indicating the separase sensor ratio in securin MO + separase AA oocytes (*n* = 10). Quantification of separase sensor cleavage minimum in control (green crosses, *n* = 28), SGO2 MO (purple crosses, *n* = 7), SGO2 MO + securin MO (orange crosses, *n* = 9), SGO2 MO + separase AA (blue crosses, *n* = 11), and SGO2 + securin MO + separase AA (burgundy crosses, *n* = 9) oocytes. Crosses represent individual oocytes. **(c)** Quantification of polar body extrusion timings in oocyte treatment groups shown in panel **(b)**. Timings are relative to the mean polar body extrusion time (0) in control oocytes. **(d)** Representative images showing chromosome alignment and segregation in **(i)** control, **(ii)** SGO2 MO, **(iii)** SGO2 + securin MO, **(iv)** SGO2 MO + separase AA, and **(v)** SGO2 + securin MO + separase AA oocytes. Time relative to PB1 extrusion. Chromosomes were visualized by incubating oocytes with SiR-DNA (magenta). Scale bar = 10 μm. **(e)** Quantification of chromosome alignment length, measured axial to the spindle per 10-min time points over 4 h prior to PB1 extrusion. Comparing control oocytes (green traces, *n* = 9) with **(i)** SGO2 MO (purple trace, *n* = 5), **(ii)** SGO2 MO + securin MO (orange trace, *n* = 7), **(iii)** SGO2 MO + separase AA (blue trace, *n* = 7), and **(iv)** SGO2 + securin MO + separase WT oocytes (burgundy trace, *n* = 7). In part (iv) a dashed dark blue line is included for comparison, indicating chromosome alignment in securin MO + separase AA oocytes (*n* = 7). **(f)** Quantification of chromosome alignment length 1 h before PB1 extrusion in treatment groups as shown in panel (e). Crosses represent individual oocyte measurements. In panels (a) and (e): thick lines show the mean data, lighter shadows show the SEM. In panels (b), (c), and (f): ****$P < 0.0001$, ***$P < 0.001$, **$P < 0.01$, *$P < 0.1$, n.s. = non-significant, two-sided unpaired *t* test; box = 25%–75%, whiskers = 0%–100%, center = median, center box = mean. All source data can be found in the S1 Data spreadsheet.

https://doi.org/10.1371/journal.pbio.3003131.g003

of securin results in loss of sister chromatid cohesion and subsequent segregation errors [45,46]. Separase must therefore be carefully regulated through the MI-MII transition, perhaps explaining the existence of compensatory mechanisms of separase inhibition.

In the current study, we demonstrate that exogenous SGO2 is targeted for degradation by the APC/C in anaphase I, after cyclin B1 and securin, where destruction initiates in prometaphase I. Initially, it seemed plausible that SGO2 may act as a late inhibitor of separase in oocytes. However, severe SGO2 depletion alone does not impact the timing of separase release, and SGO2 depletion in securin MO + separase AA oocytes neither alters the timing of sensor cleavage nor exacerbates defects in chromosome alignment and segregation. In addition, it is perhaps counterintuitive for SGO2 to act as a separase inhibitor in mouse oocytes, since direct SGO2-MAD2 binding has previously been demonstrated to be important for SAC silencing during meiosis I [47]. SGO2-MAD2 thereby promotes securin and cyclin B1 destruction to activate, rather than inhibit, separase. A recent study also demonstrated that MAD2 is dispensable for accurate chromosome segregation in mouse oocytes using mice with an oocyte-specific depletion of MAD2 [48]. We suggest that in a healthy oocyte, it is not necessary for SGO2 to play a separase inhibitory role, and that in an aging context, the depletion of SGO2 and MAD2 makes it less likely that any inhibitory contribution would be meaningful [49–51].

A caveat to our study is that our methods relied on the use of MOs, which, while severely depleting securin and SGO2, leave some residual protein. Nevertheless, limiting both cyclin B1-CDK1-mediated and securin-mediated separase inhibition accelerates separase release by ~1 h. But what inhibits separase before this time point? Notably, initiation of separase release is still acute in this double perturbation context, and this is important. While it seems unlikely that SGO2 takes on this role (SGO2 depletion has no additive impact), it is possible that an unknown separase inhibitor acts over this time period. A characteristic of this inhibitor would be its loss, inactivation, or relocalisation ~1.5 h ahead of polar body extrusion; currently uncharacterized SGO2 isotypes present possible candidates. However, we propose an alternative and suggest that this is more likely. In securin MO + separase AA oocytes, our data and that of others strongly suggest that endogenous cyclin-CDK1 is sufficient to inhibit all endogenous separase activity. Most convincingly, female mice devoid of securin are fertile [52,53]. In this context, our experimental oocytes are then only vulnerable to exogenous separase AA, which might not be in excess of even very reduced levels of securin in securin MO oocytes. It is plausible that residual securin is sufficient to inhibit separase AA up to a tipping point that is reached earlier in these oocytes when compared to control oocytes with high levels of securin. The period of separase inhibition beyond the initiation of cyclin B1 and securin destruction ~2.5 h ahead of polar body extrusion, is then directly governed by their availability. In line with this, an elegant pre-print published during the revisions of this manuscript showed that when separase activity is rescued using the S1126A mutant in separase$^{-/-}$ securin$^{-/-}$ mouse oocytes, separase sensor cleavage begins soon after NEBD [54]. Importantly, this study also provides independent validation that SGO2 is not essential for separase control during oocyte meiosis.

A second important question raised by our findings is why there are such pronounced alignment defects in securin MO + separase AA (and SGO2 MO + securin MO + separase AA) oocytes, hours before detectable separase activity. In these oocytes, chromosomes are disorganized from initial spindle assembly compared to controls. We suggest that this impact is also related to the addition of separase AA since mRNA is microinjected into GV-stage oocytes. At this time point in unperturbed oocytes, endogenous securin, and separase levels are low. In our experimental setting, we shift the balance toward substantially reduced securin (due to prior securin MO addition), but generate separase that cannot be inhibited by cyclin B1-CDK1. Following meiosis I resumption, as spindle assembly initiates, it is plausible that there is aberrant early separase activity, which could result in chromosome architecture damage from the outset. This would be difficult to detect, as the H2B-targeted separase sensor does not become discretely localized until after chromosome condensation.

Given its known role in protecting centromeric cohesion in oocytes [55,56], one might expect that the removal of SGO2 would result in segregation defects. However, this was not detectable in our study. In SGO2-depleted (SGO2 MO) oocytes, as well as in SGO2 MO + securin MO and SGO2 MO + separase AA oocytes, separase activation occurs at the same time as in control oocytes, and chromosomes segregate correctly. Interestingly however, in oocytes where SGO2 was removed in a securin MO + separase AA background (SGO2 MO + securin MO + separase AA), total cleavage of the separase sensor was significantly reduced, and polar body extrusion was delayed. This is in contrast to securin MO + separase AA oocytes, where the total cleavage of the sensor was substantially higher than in control oocytes. While this may potentially be due to improper folding of newly synthesized separase through loss of interaction with its inhibitory partners, we suggest this is unlikely due to the pronounced cleavage profile in securin MO + separase AA oocytes. We instead propose that this is specific to the loss of SGO2 and its previously described role in silencing the SAC during meiosis I in oocytes [57]. In securin MO + separase AA oocytes, the severe errors in chromosome alignment are expected to result in residual high SAC activity later into meiosis compared to controls. When this high SAC activity is coupled with the removal of SGO2, as in SGO2 MO + securin MO + separase AA oocytes, the inability to efficiently deactivate the SAC may hinder APC/C-mediated degradation of securin and cyclin B1. This would result in reduced separase activation, and the reduced sensor cleavage and delayed polar body extrusion observed in these oocytes. It is important to also note here that in a small percentage SGO2 + securin MO + separase AA oocytes, the alignment and segregation errors are so severe that polar body extrusion fails completely.

To conclude, our results demonstrate that either securin- or cyclin B1-CDK1-mediated inhibition is independently sufficient to suppress separase during meiosis I in oocytes. In contrast, when these compensatory pathways are perturbed in tandem, separase activity begins up to 1.5 h ahead of polar body extrusion and is accompanied by gross segregation defects. This erroneous phenotype is not exacerbated when SGO2 protein levels are also depleted. Compensatory pathways of separase inhibition may have multiple advantages, some of which are discussed above but also include changes that take place during oocyte aging. Here, the protein balance in the oocyte shifts towards an increased risk of aberrant separase activity; greater numbers of separase transcripts are observed [58], while the APC/C becomes more active during anaphase I, destroying greater quantities of securin [45]. In addition, aged oocytes have decreased levels of SAC proteins [45,59–61], and a diminished population of both SGO2 and cohesin that act to maintain homologous chromosome architecture during meiosis I [62–67].

This work highlights another example of the oocyte's ability to adapt to the unique challenges presented during this specialized cell division.

Methods

Oocyte collection and culture

Six- to twelve-week-old female, outbred, CD1 mice (Charles River) were used. All animals were handled in accordance with ethics approved by the UK Home Office Animals Scientific Procedures Act 1986. However, given that mice did not undergo a 'procedure' as defined by the Act, the project did not require Home Office Licensing. The reason for animal use

was instead approved and governed by Newcastle University's Comparative Biology Centre Ethics Committee; AWERB Approval Reference Number; 663. GV stage oocytes were collected from ovaries punctured with a sterile needle and stripped of their cumulus cells mechanically using a pipette. For bench handling, microinjections, and imaging experiments, oocytes were cultured at 37 °C in M2 medium (Sigma Aldrich) supplemented with Penicillin-Streptomycin and where necessary with the addition of 30 nM 3-isobutyl-1-methylxanthine (Sigma Aldrich) to arrest oocytes at prophase I. Data were only collected from oocytes that underwent NEBD with normal timings and had a diameter within 95%–105% of the population average. Where destruction profiles are displayed, *n* is the number of oocytes from which the data have been gathered. Oocyte datasets were typically gathered from three independent experiments. For each independent experiment, both control and treatment groups were derived from the same pool of oocytes, collected from a minimum of two animals. Oocytes were selected at random for microinjection.

Preparation of mRNA constructs for microinjection

H2B-mScarlet- hRec8(297-506)-mNeonGreen was a gift from Iain Cheeseman (Addgene plasmid # 174717; http://n2t.net/addgene:174717; RRID:Addgene_174717) [68]. Separase AA and the Scc1 and Rec8 separase sensors were constructed in pRN3 vectors as described previously [26]. Mouse *Sgo2la* cDNA (a gift from Mary Herbert) was amplified, and mutations were inserted, by primer overhang extension PCR. Following this, wild-type and mutant SGO2 were inserted into a modified pRN3 vector designed to produce mRNA transcripts C-terminally coupled to mVenus [69] using NEBuilder (New England Biolabs). Resultant plasmids were linearized and mRNA for microinjection was prepared using a T3 mMESSAGE mMACHINE kit (Ambion) according to the manufacturer's instructions. mRNA was dissolved in nuclease-free water to the required micropipette concentration.

Knockdown of gene expression by morpholino oligo

Morpholino antisense oligos designed to recognize the 5′-UTR of mouse securin (sequence: GATAAGAGTAGCCATTCTGGATTAC; MO; Gene Tools) or SGO2 (sequence: CTGAAAACTAGTGGCGACCCCTCGC; MO; Gene Tools) were used to knock down gene expression. As per the manufacturer's instructions, the oligo was stored at room temperature, heated for 5 min at 65 °C prior to use, and injected at a micropipette concentration of 1 mM. Morpholinos stored in suspension for extended periods of time were autoclaved prior to use. All morpholinos were injected with sufficient time for protein turnover to result in an effective knock-down as quantified by western blot for securin [26] and by immunofluorescence for SGO2 (S2 Fig).

Microinjection

Oocyte microinjection of the MO and construct mRNAs was carried out on the heated stage of an inverted microscope fitted for epifluorescence (Olympus; IX71). In brief, micropipettes fabricated using a P-97 (Sutter Instruments) were inserted into cells using the negative capacitance overcompensation facility on an electrophysiological amplifier (World Precision Instruments). This procedure ensures a high rate of oocyte survival (>95%). The final volume of injection was estimated by the diameter of displaced ooplasm and was typically between 0.1% and 0.3% of total volume.

Immunofluorescence

Cumulus-free oocytes synchronized in meiosis I by IMBX washout were attached to 8-well chamber slides using Cell-Tak (Corning) (all experimental groups were fixed and stained in the same well). Oocytes were washed with warm phosphate-buffered saline (PBS, Gibco) before being fixed for 30 min at room temperature in PBS containing 1.6% formaldehyde (Sigma Aldrich) and 0.1% Triton X-100 (Thermo Scientific). Following fixation, oocytes were further permeabilised in PBS containing 0.1% Triton X-100 at 4 °C overnight before being washed into PBS containing 0.1% Tween (Sigma Aldrich) for storage of up to 2 days. Oocytes were blocked in 3% w/v Bovine Serum Albumin (BSA, Sigma Aldrich) PBS-Tween for

1–2 h at room temperature, before incubating at 4 °C overnight with primary antibodies. SGO2 knockdown was assayed with a polyclonal rabbit antibody from Biorbyt (orb499806, Lot: BS67182) used at 1:1000 in 3% BSA PBS-Tween. After 3× 5-min washes in 3% BSA PBS-Tween, oocytes were incubated with donkey anti-rabbit Alexa Fluor Plus secondary antibodies at 1:1000 (Invitrogen). Samples were then washed twice with PBS-Tween and once with PBS before imaging.

Microscopy

For all live-cell imaging, the far-red fluorescent DNA-intercalator SiR-DNA (Spirochrome) was added to the culture media 30 min prior to imaging at a final concentration of 125 nM. Media was maintained at 37 °C under mineral oil. To generate destruction profiles of fluorescent constructs, Differential Interference Contrast and fluorescence Z-sections were captured every 10 min through meiosis I using a Leica DMi8 inverted microscope with a K5 sCMOS camera (Leica Microsystems) and a 10× air objective lens. Fixed-cell immunofluorescence imaging was performed at room temperature using the same microscope and a 20× air objective lens.

Confocal images (all experiments using the separase biosensor) were captured using a Zeiss LSM 800 with a 40× oil immersion objective lens. Oocytes were imaged at 10-min intervals through 20+ Z-sections over 12–15 h from 10 to 20 min NEBD. For separase sensor imaging, the laser power was adjusted so that the recorded intensity of the mCherry and eGFP channels were approximately equivalent. Transmitted light and fluorescent images were recorded in Zen Blue (Zeiss) and processed in the Fiji distribution of ImageJ [70].

Quantification and analysis

For real-time SGO2 destruction profiling, images were recorded using LasX (Leica microsystems). Fluorescence intensity was subsequently measured in Fiji by taking a total VFP intensity reading from a defined region of interest around the oocyte. Data was plotted over time per oocyte aligned at PB1 extrusion. Due to the natural variation in anaphase and polar body extrusion timing relative to NEBD between individual oocytes within the same treatment group, we were able to quantify differences in cleavage timing more accurately by aligning traces relative to polar body extrusion. Importantly, we observed no evidence of altered NEBD timings in any oocyte groups. Fluorescence data values are arbitrary. Individual data sets were normalized prior to calculating the mean so that each data set was represented equally (taking the maximum fluorescence prior to anaphase as 100 arbitrary units). However, we also compared all raw traces, confirming that in each experiment, the timing and magnitude of construct destruction remained the same, regardless of the data handling method or variation in pre-destruction fluorescence. Comparisons typically include data from oocytes with comparable reporter expression levels. All mean destruction traces have associated data sets in individual oocytes.

For measuring SGO2 knock-down in prometaphase I, a DNA clipping mask was generated using the SiR-DNA channel in Fiji. This mask was applied to the VFP channel to isolate DNA-localizing signal and exclude non-specific primary antibody staining. The intensity of DNA-localizing SGO2 signal was then measured.

Cleavage profiles for separase biosensor experiments were produced in Fiji by again creating a clipping mask of the DNA using the SiR-DNA channel. The eGFP and mCherry signals within the area defined by the clipping mask were then measured and aligned at PB1 extrusion. Oocytes that did not undergo PB1 extrusion could not be aligned and were therefore excluded. eGFP/mCherry ratios were calculated in Excel. When plotting construct destruction traces or separase sensor ratios, for clarity, only the mean trace is shown with SEM error bars. For measuring chromosome alignment length, a maximum intensity projection of the SiR-DNA channel was produced in Fiji, and the distance between the furthest edges of the chromosomes was measured axial to the spindle.

Multiple sequence alignments

Sequence conservation alignments were made by importing protein sequences from Uniprot and aligning in Jalview [71], version 15.0. The full sequence alignment conservation annotation shown in Fig 2a is between SGO2 orthologs from

Homo sapiens, *Mus musculus*, *Rattus norvegicus*, *Bos Taurus*, *Sus domesticus*, *Rhinolophus ferrumequinum*, and *Trachemys scripta elegans*. All figures were prepared in Adobe Illustrator CC, version 17.1.0.

Supporting information

S1 Fig. Separase sensor cleavage is detected earlier in oocytes where both securin and cyclin B1-CDK1 inhibitory pathways are restricted. (a) Schematic diagram showing the H2B-mCherry-hScc1-eGFP separase sensor. **(b)** Representaive images of **(i)** control and **(ii)** securin MO + separase AA oocytes at 10-min intervals over 1 h prior to PB1 extrusion. Panels show the mCherry signal which remains histone-bound, the eGFP signal which dissociates into the cytoplasm on sensor cleavage, and their overlay. Notably in (ii), securin MO + separase AA oocytes, the eGFP signal begins to decrease approximately 30 min earlier than in (i), control oocytes. In this example, the majority of chromosomes are extruded in the polar body.
(TIF)

S2 Fig. Quantification of shugoshin-2 (SGO2) knockdown by morpholino oligo (MO). (a) Representative images of control and SGO2 MO oocytes collected at 3 h post-NEBD and immunostained for SGO2. **(b)** Quantification of SGO2 protein levels in control (green crosses, $n = 6$) and SGO2 MO (magenta crosses, $n = 8$) oocytes normalized to the mean SGO2 protein level in control oocytes. In panel (b): ****$P < 0.0001$, ***$P <$ 0. 001, **$P < 0.01$, *$P < 0.1$, n.s. = non-significant. Significance was calculated by unpaired *t* test. All source data can be found in the S1 Data spreadsheet.
(TIF)

S1 Data. Source data—Excel spreadsheet containing source data for all figures.
(XLSX)

Acknowledgments

We would also like to thank Glyn Nelson (Bioimaging Unit, Faculty of Medical Sciences, Newcastle University) for his invaluable help with imaging.

Author contributions

Conceptualization: Christopher Thomas, Suzanne Madgwick.

Formal analysis: Benjamin Wetherall, Christopher Thomas, Suzanne Madgwick.

Funding acquisition: Suzanne Madgwick.

Investigation: Benjamin Wetherall, David Bulmer, Alexandra Sarginson, Christopher Thomas, Suzanne Madgwick.

Methodology: Benjamin Wetherall, Christopher Thomas, Suzanne Madgwick.

Supervision: Suzanne Madgwick.

Writing – original draft: Benjamin Wetherall, Christopher Thomas, Suzanne Madgwick.

Writing – review & editing: Benjamin Wetherall, Christopher Thomas, Suzanne Madgwick.

References

1. Webster A, Schuh M. Mechanisms of aneuploidy in human eggs. Trends Cell Biol. 2017;27(1):55–68. https://doi.org/10.1016/j.tcb.2016.09.002 PMID: 27773484
2. Watanabe Y, Nurse P. Cohesin Rec8 is required for reductional chromosome segregation at meiosis. Nature. 1999;400(6743):461–4. https://doi.org/10.1038/22774 PMID: 10440376
3. Duro E, Marston AL. From equator to pole: splitting chromosomes in mitosis and meiosis. Genes Dev. 2015;29(2):109–22. https://doi.org/10.1101/gad.255554.114 PMID: 25593304

4. Uhlmann F, Wernic D, Poupart MA, Koonin EV, Nasmyth K. Cleavage of cohesin by the CD clan protease separin triggers anaphase in yeast. Cell. 2000;103(3):375–86. https://doi.org/10.1016/s0092-8674(00)00130-6 PMID: 11081625
5. Hauf S, Waizenegger IC, Peters JM. Cohesin cleavage by separase required for anaphase and cytokinesis in human cells. Science. 2001;293(5533):1320–3. https://doi.org/10.1126/science.1061376 PMID: 11509732
6. Kudo NR, Wassmann K, Anger M, Schuh M, Wirth KG, Xu H, et al. Resolution of chiasmata in oocytes requires separase-mediated proteolysis. Cell. 2006;126(1):135–46. https://doi.org/10.1016/j.cell.2006.05.033 PMID: 16839882
7. Waizenegger I, Giménez-Abián JF, Wernic D, Peters J-M. Regulation of human separase by securin binding and autocleavage. Curr Biol. 2002;12(16):1368–78. https://doi.org/10.1016/s0960-9822(02)01073-4 PMID: 12194817
8. Yu J, Morgan DO, Boland A. The molecular mechanisms of human separase regulation. Biochem Soc Trans. 2023;51(3):1225–33. https://doi.org/10.1042/BST20221400 PMID: 37140261
9. Boland A, Martin TG, Zhang Z, Yang J, Bai X-C, Chang L, et al. Cryo-EM structure of a metazoan separase-securin complex at near-atomic resolution. Nat Struct Mol Biol. 2017;24(4):414–8. https://doi.org/10.1038/nsmb.3386 PMID: 28263324
10. Yu J, Raia P, Ghent CM, Raisch T, Sadian Y, Cavadini S, et al. Structural basis of human separase regulation by securin and CDK1-cyclin B1. Nature. 2021;596(7870):138–42. https://doi.org/10.1038/s41586-021-03764-0 PMID: 34290405
11. Luo S, Tong L. Structural biology of the separase–securin complex with crucial roles in chromosome segregation. Curr Opin Struct Biol. 2018;49:114–22.
12. Luo S, Tong L. Molecular mechanism for the regulation of yeast separase by securin. Nature. 2017;542(7640):255–9. https://doi.org/10.1038/nature21061 PMID: 28146474
13. Nagao K, Yanagida M. Securin can have a separase cleavage site by substitution mutations in the domain required for stabilization and inhibition of separase. Genes Cells. 2006;11(3):247–60. https://doi.org/10.1111/j.1365-2443.2006.00941.x PMID: 16483313
14. Stemmann O, Zou H, Gerber SA, Gygi SP, Kirschner MW. Dual inhibition of sister chromatid separation at metaphase. Cell. 2001;107(6):715–26. https://doi.org/10.1016/s0092-8674(01)00603-1 PMID: 11747808
15. Gorr IH, Boos D, Stemmann O. Mutual inhibition of separase and Cdk1 by two-step complex formation. Mol Cell. 2005;19(1):135–41. https://doi.org/10.1016/j.molcel.2005.05.022 PMID: 15989971
16. Stemmann O, Gorr IH, Boos D. Anaphase topsy-turvy: Cdk1 a securin, separase a CKI. Cell Cycle. 2006;5(1):11–3. https://doi.org/10.4161/cc.5.1.2296 PMID: 16340311
17. Holland AJ, Taylor SS. Cyclin-B1-mediated inhibition of excess separase is required for timely chromosome disjunction. J Cell Sci. 2006;119(Pt 16):3325–36. https://doi.org/10.1242/jcs.03083 PMID: 16868023
18. Nabti I, Reis A, Levasseur M, Stemmann O, Jones KT. Securin and not CDK1/cyclin B1 regulates sister chromatid disjunction during meiosis II in mouse eggs. Dev Biol. 2008;321(2):379–86. https://doi.org/10.1016/j.ydbio.2008.06.036 PMID: 18639540
19. Huang X, Andreu-Vieyra CV, Wang M, Cooney AJ, Matzuk MM, Zhang P. Preimplantation mouse embryos depend on inhibitory phosphorylation of separase to prevent chromosome missegregation. Mol Cell Biol. 2009;29(6):1498–505. https://doi.org/10.1128/MCB.01778-08 PMID: 19124608
20. Kamenz J, Hauf S. Time to split up: dynamics of chromosome separation. Trends Cell Biol. 2017;27(1):42–54. https://doi.org/10.1016/j.tcb.2016.07.008 PMID: 27567180
21. Mei J, Huang X, Zhang P. Securin is not required for cellular viability, but is required for normal growth of mouse embryonic fibroblasts. Curr Biol. 2001;11(15):1197–201. https://doi.org/10.1016/s0960-9822(01)00325-6 PMID: 11516952
22. Pfleghaar K., Heubes S., Cox J., Stemmann O. & Speicher M. R. Securin is not required for chromosomal stability in human cells. PLoS Biol 3, 1–8 (2005).
23. Wirth KG, Wutz G, Kudo NR, Desdouets C, Zetterberg A, Taghybeeglu S, et al. Separase: a universal trigger for sister chromatid disjunction but not chromosome cycle progression. J Cell Biol. 2006;172(6):847–60. https://doi.org/10.1083/jcb.200506119 PMID: 16533945
24. Chiang T, Schultz RM, Lampson MA. Age-dependent susceptibility of chromosome cohesion to premature separase activation in mouse oocytes. Biol Reprod. 2011;85(6):1279–83. https://doi.org/10.1095/biolreprod.111.094094 PMID: 21865557
25. Hellmuth S, Gómez-H L, Pendás AM, Stemmann O. Securin-independent regulation of separase by checkpoint-induced shugoshin-MAD2. Nature. 2020;580(7804):536–41. https://doi.org/10.1038/s41586-020-2182-3 PMID: 32322060
26. Thomas C, Wetherall B, Levasseur MD, Harris RJ, Kerridge ST, Higgins JMG, et al. A prometaphase mechanism of securin destruction is essential for meiotic progression in mouse oocytes. Nat Commun. 2021;12(1):4322. https://doi.org/10.1038/s41467-021-24554-2 PMID: 34262048
27. Levasseur MD, Thomas C, Davies OR, Higgins JMG, Madgwick S. Aneuploidy in oocytes is prevented by sustained CDK1 activity through degron masking in cyclin B1. Developmental Cell. 2019;48(5):672-684.e5. https://doi.org/10.1016/j.devcel.2019.01.002
28. Nam H-J, van Deursen JM. Cyclin B2 and p53 control proper timing of centrosome separation. Nat Cell Biol. 2014;16(6):538–49. https://doi.org/10.1038/ncb2952 PMID: 24776885
29. Rosen LE, Klebba JE, Asfaha JB, Ghent CM, Campbell MG, Cheng Y, et al. Cohesin cleavage by separase is enhanced by a substrate motif distinct from the cleavage site. Nat Commun. 2019;10(1):5189. https://doi.org/10.1038/s41467-019-13209-y PMID: 31729382
30. Shindo N, Kumada K, Hirota T. Separase sensor reveals dual roles for separase coordinating cohesin cleavage and cdk1 inhibition. Dev Cell. 2012;23(1):112–23. https://doi.org/10.1016/j.devcel.2012.06.015 PMID: 22814604

31. Nikalayevich E, Bouftas N, Wassmann K. Detection of separase activity using a cleavage sensor in live mouse oocytes. Methods Mol Biol. 2018;1818:99–112. https://doi.org/10.1007/978-1-4939-8603-3_11 PMID: 29961259
32. Touati SA, Wassmann K. How oocytes try to get it right: spindle checkpoint control in meiosis. Chromosoma. 2016;125(2):321–35. https://doi.org/10.1007/s00412-015-0536-7 PMID: 26255654
33. Clute P, Pines J. Temporal and spatial control of cyclin B1 destruction in metaphase. Nat Cell Biol. 1999;1(2):82–7. https://doi.org/10.1038/10049 PMID: 10559878
34. Zur A, Brandeis M. Securin degradation is mediated by fzy and fzr, and is required for complete chromatid separation but not for cytokinesis. EMBO J. 2001;20(4):792–801. https://doi.org/10.1093/emboj/20.4.792 PMID: 11179223
35. Karamysheva Z, Diaz-Martinez LA, Crow SE, Li B, Yu H. Multiple anaphase-promoting complex/cyclosome degrons mediate the degradation of human Sgo1. J Biol Chem. 2009;284(3):1772–80. https://doi.org/10.1074/jbc.M807083200 PMID: 19015261
36. Davey NE, Morgan DO. Building a regulatory network with short linear sequence motifs: lessons from the degrons of the anaphase-promoting complex. Mol Cell. 2016;64(1):12–23. https://doi.org/10.1016/j.molcel.2016.09.006 PMID: 27716480
37. Pfleger CM, Kirschner MW. The KEN box: an APC recognition signal distinct from the D box targeted by Cdh1. Genes Dev. 2000;14(6):655–65. https://doi.org/10.1101/gad.14.6.655 PMID: 10733526
38. Jin L, Williamson A, Banerjee S, Philipp I, Rape M. Mechanism of ubiquitin-chain formation by the human anaphase-promoting complex. Cell. 2008;133(4):653–65. https://doi.org/10.1016/j.cell.2008.04.012 PMID: 18485873
39. Glotzer M, Murray AW, Kirschner MW. Cyclin is degraded by the ubiquitin pathway. Nature. 1991;349(6305):132–8. https://doi.org/10.1038/349132a0 PMID: 1846030
40. Herbert M, Levasseur M, Homer H, Yallop K, Murdoch A, McDougall A. Homologue disjunction in mouse oocytes requires proteolysis of securin and cyclin B1. Nat Cell Biol. 2003;5(11):1023–5. https://doi.org/10.1038/ncb1062 PMID: 14593421
41. Adhikari D, Zheng W, Shen Y, Gorre N, Ning Y, Halet G, et al. Cdk1, but not Cdk2, is the sole Cdk that is essential and sufficient to drive resumption of meiosis in mouse oocytes. Hum Mol Genet. 2012;21(11):2476–84. https://doi.org/10.1093/hmg/dds061 PMID: 22367880
42. Diril MK, Ratnacaram CK, Padmakumar VC, Du T, Wasser M, Coppola V, et al. Cyclin-dependent kinase 1 (Cdk1) is essential for cell division and suppression of DNA re-replication but not for liver regeneration. Proc Natl Acad Sci U S A. 2012;109(10):3826–31. https://doi.org/10.1073/pnas.1115201109 PMID: 22355113
43. Waizenegger I, Giménez-Abián JF, Wernic D, Peters J-M. Regulation of human separase by securin binding and autocleavage. Curr Biol. 2002;12(16):1368–78. https://doi.org/10.1016/s0960-9822(02)01073-4 PMID: 12194817
44. Bouftas N, Wassmann K. Cycling through mammalian meiosis: B-type cyclins in oocytes. Cell Cycle. 2019;18(14):1537–48. https://doi.org/10.1080/15384101.2019.1632139 PMID: 31208271
45. Nabti I, Grimes R, Sarna H, Marangos P, Carroll J. Maternal age-dependent APC/C-mediated decrease in securin causes premature sister chromatid separation in meiosis II. Nat Commun. 2017;8(1):1–9.
46. Wassmann K. Separase control and cohesin cleavage in oocytes: should I stay or should I go?. Cells. 2022;11.
47. Rattani A, Wolna M, Ploquin M, Helmhart W, Morrone S, Mayer B, et al. Sgol2 provides a regulatory platform that coordinates essential cell cycle processes during meiosis I in oocytes. Elife. 2013;2:e01133. https://doi.org/10.7554/eLife.01133 PMID: 24192037
48. Qiao J-Y, Zhou Q, Xu K, Yue W, Lei W-L, Li Y-Y, et al. Mad2 is dispensable for accurate chromosome segregation but becomes essential when oocytes are subjected to environmental stress. Development. 2023;150(14):dev201398. https://doi.org/10.1242/dev.201398 PMID: 37485540
49. Steuerwald NM, Steuerwald MD, Mailhes JB. Post-ovulatory aging of mouse oocytes leads to decreased MAD2 transcripts and increased frequencies of premature centromere separation and anaphase. Mol Hum Reprod. 2005;11(9):623–30. https://doi.org/10.1093/molehr/gah231 PMID: 16207798
50. Lister LM, Kouznetsova A, Hyslop LA, Kalleas D, Pace SL, Barel JC, et al. Age-related meiotic segregation errors in mammalian oocytes are preceded by depletion of cohesin and Sgo2. Curr Biol. 2010;20(17):1511–21. https://doi.org/10.1016/j.cub.2010.08.023 PMID: 20817533
51. Mihalas BP, et al. Age-dependent loss of cohesion protection in human oocytes. Curr Biol. 2024;34:117-131.e5.
52. Mei J, Huang X, Zhang P. Securin is not required for cellular viability, but is required for normal growth of mouse embryonic fibroblasts. Curr Biol. 2001;11(15):1197–201. https://doi.org/10.1016/s0960-9822(01)00325-6 PMID: 11516952
53. Wang Z, Yu R, Melmed S. Mice lacking pituitary tumor transforming gene show testicular and splenic hypoplasia, thymic hyperplasia, thrombocytopenia, aberrant cell cycle progression, and premature centromere division. Mol Endocrinol. 2001;15(11):1870–9. https://doi.org/10.1210/mend.15.11.0729 PMID: 11682618
54. Jailani SE, Cladière D, Nikalayevich E, Touati SA, Chesnokova V, Melmed S, et al. Elimination of separase inhibition reveals absence of cohesin protection in oocyte metaphase II. 2025. https://doi.org/10.1101/2025.02.11.637638
55. Lee J, Kitajima TS, Tanno Y, Yoshida K, Morita T, Miyano T, et al. Unified mode of centromeric protection by shugoshin in mammalian oocytes and somatic cells. Nat Cell Biol. 2008;10(1):42–52. https://doi.org/10.1038/ncb1667 PMID: 18084284
56. El Yakoubi W, Buffin E, Cladière D, Gryaznova Y, Berenguer I, Touati SA, et al. Mps1 kinase-dependent Sgo2 centromere localisation mediates cohesin protection in mouse oocyte meiosis I. Nat Commun. 2017;8(1):694. https://doi.org/10.1038/s41467-017-00774-3 PMID: 28947820
57. Rattani A, Wolna M, Ploquin M, Helmhart W, Morrone S, Mayer B, et al. Sgol2 provides a regulatory platform that coordinates essential cell cycle processes during meiosis I in oocytes. Elife. 2013;2:e01133. https://doi.org/10.7554/eLife.01133 PMID: 24192037

58. Yuan L, Yin P, Yan H, Zhong X, Ren C, Li K, et al. Single-cell transcriptome analysis of human oocyte ageing. J Cell Mol Med. 2021;25(13):6289–303. https://doi.org/10.1111/jcmm.16594 PMID: 34037315

59. Pan H, Ma P, Zhu W, Schultz RM. Age-associated increase in aneuploidy and changes in gene expression in mouse eggs. Dev Biol. 2008;316(2):397–407. https://doi.org/10.1016/j.ydbio.2008.01.048 PMID: 18342300

60. Riris S, Webster P, Homer H. Digital multiplexed mRNA analysis of functionally important genes in single human oocytes and correlation of changes in transcript levels with oocyte protein expression. Fertil Steril. 2014;101(3):857–64. https://doi.org/10.1016/j.fertnstert.2013.11.125 PMID: 24444598

61. Steuerwald N., Cohen J., Herrera R. J., Sandalinas M. & Brenner C. A. Association between spindle assembly checkpoint expression and maternal age in human oocytes. Mol Hum Reprod 7, 49–55 (2001).

62. Lister LM, Kouznetsova A, Hyslop LA, Kalleas D, Pace SL, Barel JC, et al. Age-related meiotic segregation errors in mammalian oocytes are preceded by depletion of cohesin and Sgo2. Curr Biol. 2010;20(17):1511–21. https://doi.org/10.1016/j.cub.2010.08.023 PMID: 20817533

63. Chiang T, Duncan FE, Schindler K, Schultz RM, Lampson MA. Evidence that weakened centromere cohesion is a leading cause of age-related aneuploidy in oocytes. Curr Biol. 2010;20(17):1522–8. https://doi.org/10.1016/j.cub.2010.06.069 PMID: 20817534

64. Tachibana-Konwalski K, Godwin J, van der Weyden L, Champion L, Kudo NR, Adams DJ, et al. Rec8-containing cohesin maintains bivalents without turnover during the growing phase of mouse oocytes. Genes Dev. 2010;24(22):2505–16. https://doi.org/10.1101/gad.605910 PMID: 20971813

65. Jessberger R. Age-related aneuploidy through cohesion exhaustion. EMBO Rep. 2012;13(6):539–46. https://doi.org/10.1038/embor.2012.54 PMID: 22565322

66. Burkhardt S, Borsos M, Szydlowska A, Godwin J, Williams SA, Cohen PE, et al. Chromosome cohesion established by Rec8-cohesin in fetal oocytes is maintained without detectable turnover in oocytes arrested for months in mice. Curr Biol. 2016;26(5):678–85. https://doi.org/10.1016/j.cub.2015.12.073 PMID: 26898469

67. Liu L, Keefe DL. Defective cohesin is associated with age-dependent misaligned chromosomes in oocytes. Reprod Biomed Online. 2008;16(1):103–12. https://doi.org/10.1016/s1472-6483(10)60562-7 PMID: 18252055

68. Maier NK, Ma J, Lampson MA, Cheeseman IM. Separase cleaves the kinetochore protein Meikin at the meiosis I/II transition. Dev Cell. 2021;56:2192-2206.e8.

69. Levasseur M. Making cRNA for microinjection and expression of fluorescently tagged proteins for live-cell imaging in oocytes. Methods Mol Biol. 2013;957:121–34. https://doi.org/10.1007/978-1-62703-191-2_8 PMID: 23138948

70. Schindelin J, Arganda-Carreras I, Frise E, Kaynig V, Longair M, Pietzsch T, et al. Fiji: an open-source platform for biological-image analysis. Nat Methods. 2012;9(7):676–82. https://doi.org/10.1038/nmeth.2019 PMID: 22743772

71. Waterhouse AM, Procter JB, Martin DMA, Clamp M, Barton GJ. Jalview Version 2—a multiple sequence alignment editor and analysis workbench. Bioinformatics. 2009;25(9):1189–91. https://doi.org/10.1093/bioinformatics/btp033 PMID: 19151095